INTERNATIONAL JOURNAL OF RECENT TRENDS IN ENGINEERING & RESEARCH
Impact Factor 4.101 ISSN -2455-1457
RECENT ADVANCES IN ELECTRONICS & COMMUNICATION ENGINEERING (RAECE-2K17)

A Power Regulation and Harmonic Current Elimination Approach for Parallel Multi-Inverter Supplying IPT Systems

B C.Premkumar
Professor, ECE
NNRG, Hydrabad, TS, India

P.Subbaiah
Professor, ECE
NNRG, Hydrabad, TS, India

Suresh.D
Professor, ECE
RNSIT, ECE,Bangalore, India

ABSRACT: ***The single resonant inverter is widely employed in typical inductive power transfer (IPT) systems to generate a high-frequency current in the primary side. However, the power capacity of a single resonant inverter is limited by the constraints of power electronic devices and the relevant cost. Consequently, IPT systems fail to meet high-power application requirements, such as those in rail applications. Total harmonic distortion (THD) may also violate the standard electromagnetic interference requirements with phase shift control under light load conditions. A power regulation approach with selective harmonic elimination is proposed on the basis of a parallel multi-inverter to upgrade the power levels of IPT systems and suppress THD under light load conditions by changing the output voltage pulse width and phase shift angle among parallel multi-inverters. The validity of the proposed control approach is verified by using a 1,412.3 W prototype system, which achieves a maximum transfer efficiency of 90.602%. Output power levels can be dramatically improved with the same semiconductor capacity, and distortion can be effectively suppressed under various load conditions.***

Key words: ***Inductive power transfer (IPT), Parallel multi-inverter, Power regulation, Selective harmonic elimination***

I. INTRODUCTION

Inductive power transfer (IPT) systems are employed in many ultra-clean, ultra-dirty environments as a power provider to transfer power from the primary side to the secondary load side over a moderate air-gap distance through magnetic coupling [1]-[9] on the basis of specific application requirements. The potential advantages of IPT systems include immunity to ice, water, and other chemicals; environmental friendliness; and zero maintenance requirement. In addition, IPT systems have been adopted in a number of applications, including in the wireless charging of biomedical implants [10], mining applications [11], underwater power supply [12], electric vehicles [13]-[20], and railway applications [21],because of their ease of use, environmental sustainability, and low lifecycle cost. An IPT system is composed of a high-frequency AC power supply, a resonance tank, magnetic structures for inductive coupling, a pickup in the secondary side, and a rectifier load.

The power supply produces an alternating electric current in the primary coil, which in turn produces a time-changing magnetic field. This variable magnetic field induces an electric current (which produces a magnetic field) in the secondary solenoid windings. The induced AC and voltage are then rectified to a direct current (DC) to recharge the battery and/or the load.

Unlike consumer electronic devices, applications such as electric vehicles and rail transit systems require a large amount of power. The transferred power capacity of single inverter-based IPT systems [22]-[23] is restricted by the constraints of power electronic devices, which may be unavailable in the market or too expensive to pursue. To enhance the capacity of the resonant inverter source, the use of multiple inverters connected in parallel is proposed in [24]-[27]. A parallel connected system for induction heating based on a high-frequency inductor-capacitor-inductor (LCL) resonant inverter is described in [24]. This system requires no additional device for connecting inverters in parallel, and flexible power levels can be achieved by choosing the number of parallel inverters. A phase shift control power regulation approach for multiple LLC resonant inverters for induction heating is presented in [25] to regulate the output power of paralleled inverters by controlling the phases among them. A novel soft-switching high-frequency resonant inverter comprising two half-bridges connected in parallel is

described in [26]. By employing a new current pharos control for changing the phase shift angle between two half-bridge inverter units, the output power can be regulated continuously under a wide range of soft-switching operations. A parallel topology, which can achieve high output power levels in a cost-effective manner for IPT systems with LCL-T resonant inverters, is proposed in [27] with high reliability of functioning even when a faulty parallel H-bridge inverter is electronically shut down. However, low-order harmonics dramatically degrade the performance of some IPT systems, and such issue in harmonics is not effectively addressed by the aforementioned approaches. Safe levels of magnetic field exposure is a strict requirement for IPT systems and is a growing public concern. The maximum allowable field intensity at a given frequency related to the track current in an IPT system with an operating frequency of 20–100 kHz is provided in the guidelines [28] and does not vary with frequency. At the same time, the harmonics in the track current may increase the peak value of the track current, especially under light load conditions. Consequently, field intensity increases significantly that it violates the standards. Therefore, an approach to harmonic reduction should be developed to maintain magnetic field intensity within safe levels. A novel parallel multi-inverter IPT system is presented in the current study to upgrade the power levels of IPT systems.

The phase shift pulse width modulation method employed in parallel inverters is proposed to realize power regulation and selective harmonic elimination. The explicit solutions against phase shift angle and pulse width are given according to the constraint of the selective harmonic elimination equation and the required power to avoid solving the non-linear transcendental equation. Thus, the proposed method is suitable for real-time applications, especially for IPT systems with high operation frequency.

The remainder of this paper is organized as follows. The basic principle of the parallel multi-inverter IPT system is described in Section II. An analysis of selective harmonic elimination and output power regulation is performed by using the equivalent circuit of the proposed parallel multi-inverter IPT system in Section II. The experimental verifications on selective harmonic elimination, circulating current, and wide-ranging power regulation are carried out by using a 1,412.3 W 20 kHz prototype of an IPT system. The details are presented in Section III. The conclusion is finally drawn in Section IV.

II. BASIC PRINCIPLE OF PARALLEL MULTI-INVERTER

A. Topology Analysis of Parallel Multi- Inverter

The schematic diagram of the proposed parallel multi-inverter series-series (S-S)-tuned IPT system with voltage-fed H-bridge inverters is illustrated in Fig. 1. The inverter is composed of N identical H-bridge inverters connected in parallel. Each H-bridge inverter is connected in series to a link inductor Ln. The resonant and compensation capacitor CP is then connected in series to the parallel H-bridge inverter. The synthesized current flowing through the primary coil LP establishes magnetic coupling with the secondary coil. The secondary circuit consists of the pick-up coil LS, the compensation capacitor CS, and the load RL.

The H-bridge inverters H1 – Hn produce output voltages $u1$ – un, which are controlled by changing the phase shift angles and pulse widths in the gate pulse signals. Accordingly, the output power of each H-bridge inverter can be regulated individually. Each inverter is equipped with a protection device composed of two anti-series-connected semiconductors [29] to isolate the fault inverter from the system.

Fig. 2 shows the equivalent circuit whose resonant angular frequency is defined as

$$\omega = \frac{1}{\sqrt{L_0 C_P}} = \frac{1}{\sqrt{L_S C_S}} \qquad (1)$$

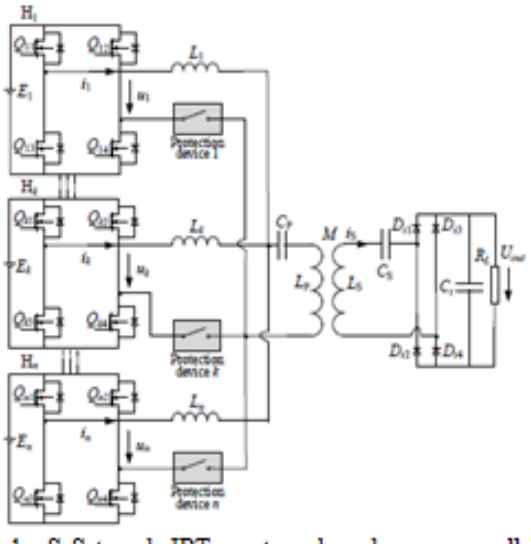

Fig. 1. S-S-tuned IPT system based on a parallel multi- inverter with protection devices.

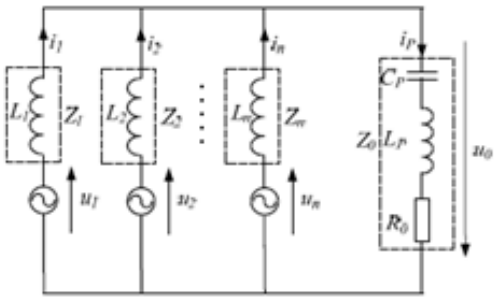

Fig. 2. Equivalent circuit of the IPT system with a parallel multi-inverter.

$$L_0 = L_P + \left(\sum_{n=1}^{N} \frac{1}{L_n} \right)^{-1} \tag{2}$$

To simplify the analysis of the operating principle of the proposed parallel multi-inverter system, we let $L_n \approx L$ and substitute (2) into (1). The operating angular frequency of the inverter can be expressed as

$$\omega = \frac{1}{\sqrt{\left(L/N + L_P\right) C_P}} \tag{3}$$

$$\begin{cases} \dot{U}_1(k) = \dot{I}_1(k) \cdot Z_1(k) + \dot{U}_0(k) \\ \vdots \\ \dot{U}_N(k) = \dot{I}_N(k) \cdot Z_N(k) + \dot{U}_0(k) \\ \dot{U}_0(k) = Z_0(k) \cdot \sum_{n=1}^{N} \dot{I}_N(k) \end{cases} \tag{4}$$

where $Z_0(k) = R_0 + jk\omega L_P + 1/(jk\omega C_P)$ $= R_0 + j\omega(NL_P k^2 - L - NL_P)/(Nk)$ and $Z_1(k) = Z_N(k) = Z_n(k) = jk\omega L = Z(k)$.

The current of each branch and the track current can be derived by

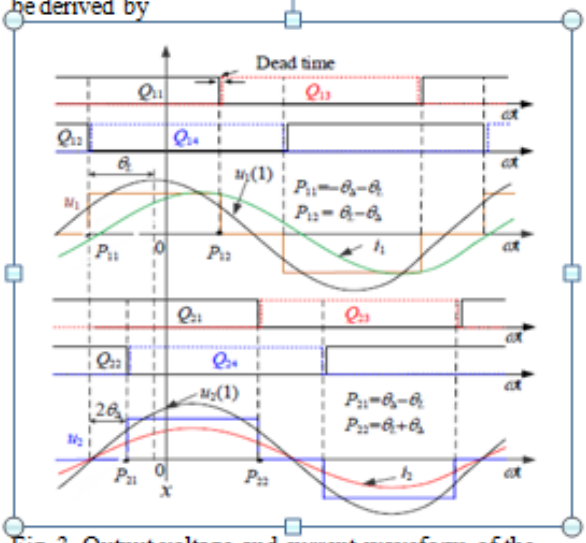

Fig. 3. Output voltage and current waveform of the inverters.

$$\dot{I}_n(k) = \frac{\left[N \cdot Z_0(k) + Z(k)\right] \cdot \dot{U}_n(k) - Z_0 \cdot \sum_{n=1}^{N} \dot{U}_n(k)}{Z(k)^2 + N \cdot Z(k) \cdot Z_0(k)} \tag{5}$$

$$\dot{I}_p(k) = \sum_{n=1}^{N} \dot{I}_n(k) = \frac{\sum_{n=1}^{N} \dot{U}_n(k)}{Z(k) + N \cdot Z_0(k)} \tag{6}$$

According to [22], the reflected impedance of the secondary circuit under resonant conditions becomes purely resistive; it can be derived by

$$R_0 = \frac{\omega^2 M^2 \pi^2}{8 R_L} \tag{7}$$

B. Topology Analysis of Parallel Multi-Inverter

1) Waveform Analysis of Voltage Source: The operating waveforms of the output voltages of the two H-bridge inverters are two identical staircases with a phase shift, as shown in Fig. 3. A coordinate system is constructed accordingly. Line x is the symmetrical center line of the staircase waveform. The origin is chosen at the point where line x and the abscissa(dt) intersect. To simplify the notation, we denote the pulse width of the staircase as 2d L and the phase shift angle between the two staircases as TS is the period of the fundamental voltage. The current changing rate caused by two parallel inverters with opposite output voltages is twice as large as that with one inverter with zero output, as shown in the following equation.

$$\frac{di}{dt} = \frac{u_1 - u_2}{L_1 + L_2} = \pm \frac{E}{L} \tag{8}$$

III. EXPERIMENTAL RESULTS

A. Prototype System

To validate the proposed approach, we construct an experimental IPT prototype in the laboratory. The prototype comprises two identical H-bridge inverters connected in parallel and is designed to operate up to 1412.3 W in the experiment. Its functions include selective harmonic elimination and power regulation by changing the output voltage pulse width and phase shift angles.

The exterior appearance of the experimental setup is shown in Fig. 9 and Fig. 10. The TMS320F28335 digital signal processing unit (DSP, Texas Instrument) is used to generate the gate pulse signals for the semi-conductors. The primary coil (L: 32 cm, W: 31.1 cm) on the bottom and the secondary coil (L: 24 cm, W: 31.1 cm) on top are made of U-shaped ferrite. The distance between the primary coil and the secondary coil is about 10 cm. The two coils are mounted to the acrylic board for mechanical support. MOSFETs (AP80N30W) and a gate driver (CONCEPT-2SC0108T2A0-17) are adopted for the H-bridge inverters. The DSP unit is utilized as the

controller of the IPT system to achieve control and protection functions among others.

The two H-bridge inverters are separately powered by two isolated DC supplies, and their AC outputs are connected in parallel to provide transmitting current in the primary coil compensated by a series capacitor. An electronic load is employed as the secondary load connected to the rectifier.

The experimental waveforms are measured and displayed by using an Agilent MSO-X 4034A scope, which allows built-in harmonic analysis. The efficiency of the system is analyzed with a YOKOGAW WT1800 power analyzer.

B. Experimental Results

To provide a clear comparison of different operating conditions, we show in Fig. 11 the experimental values of the output power, load consumption, and transmission efficiency of the IPT system against the output power.

The wide-ranging output power regulation can evidently be achieved by changing the phase shift angle and pulse width of the proposed approach and by changing the pulse width of the single inverter approach (Fig. 11). The output powers of the two inverters are approximately the same (about half of that of the single inverter approach) despite their difference resulting from the presence of a phase shift between them.

Consequently, a circulating current exists between the two inverters and results in the occurrence of a loss and a decrease in efficiency, as shown in Zones 1 and 2.

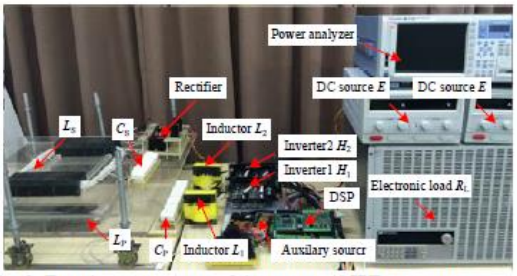

Fig. 9. Exterior appearance of the proposed IPT prototype.

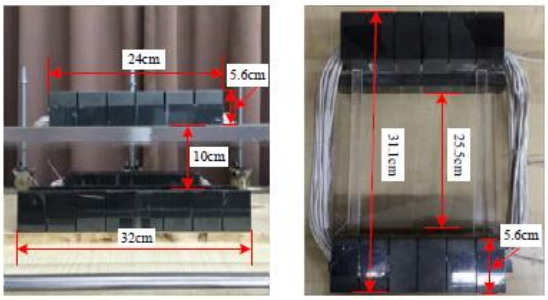

Fig. 10. Primary and secondary coils wound with a Litz wire.

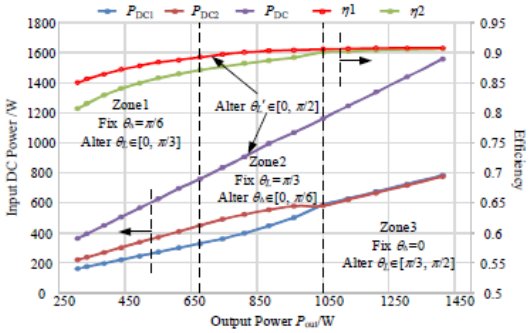

Fig. 11. Input power and overall system efficiency against the output power.

blue line (THD1) represents the THD value of the single inverter approach, and the red line (THD2) represents the THD value of the proposed algorithm. The third-, fifth-, and seventh-order harmonics are suppressed by the proposed algorithm in Zones 1 and 2 but not in Zone 3, as shown in Fig. 12(b) and (c).

Unlike the single inverter approach, the proposed algorithm can dramatically suppress the third-order harmonic of the experiment even with different DC bus voltages, as shown in Fig. 13. The output power of the experiment measured with the prototype is provided in Fig. 14. The output power can be continuously regulated from almost 0 W to 1,400 W by changing the value of d L . The comparison of the waveforms of the two approaches indicates that the proposed approach dramatically suppresses the harmonic and nearly eliminates the third-order harmonic. The same result is obtained in the

theoretical analysis. The overall efficiency of the proposed approach is about 82.9%, as shown in Fig. 15.

The waveforms of the current and voltage of the IPT system, as well as the overall efficiency (90.602%), under the maximum output power point (1,412.3 W) are shown in Fig. 16. Other working points are shown in Fig. 11.

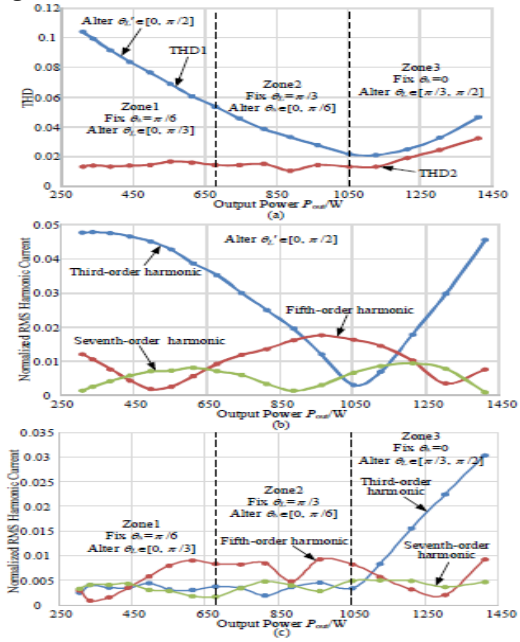

power requirements. Moreover, the output of the proposed approach involves a lower harmonic distortion under light load conditions in comparison with that of the single inverter approach. A protection scheme is provided to improve the reliability of the proposed system. The test results also show that the output voltage can be maintained to the desired value even in cases of faults, which are removed by the protection device.

REFERENCES

[1] J. T. Boys, G. A. Covic, and A. W. Green, "Stability and control of inductively coupled power transfer systems,"
IEE Proceedings - Electric Power Applications, Vol. 147, No. 1, pp. 37–43, Jan. 2000.

[2] D. J. Graham, J. A. Neasham, and B. S. Sharif, "Investigation of methods for data communication and power delivery through metals," *IEEE Trans. Ind. Electron.*, Vol. 58, No. 10, pp. 4972–4980, Oct. 2011.

[3] M. R. Amini and H. Farzanehfard, "Three-phase soft-switching inverter with minimum components," *IEEE*
Trans. Ind. Electron., Vol. 58, No. 6, pp. 2258–2264, Jun. 2011.

[4] Y. L. Li, Y. Sun, and X. Dai, "μ-Synthesis for frequency uncertainty of the ICPT system," Industrial Electronics, *IEEE Trans. Ind. Electron.*, Vol. 60, No. 1, pp. 291–300, Jan. 2013.

[5] S. Lee, B. Choi, and C. T. Rim, "Dynamics characterization of the inductive power transfer system for online electric vehicles by Laplace phasor transform," *IEEE Trans. Power Electron*., Vol. 28, No. 12, pp. 5902-5909, Dec. 2013.

[6] W. Zhang, S. C. Wong, C. K. Tse, and Q. Chen, "Analysis and comparison of secondary series- and parallel-compensated inductive power transfer systems operating for optimal efficiency and load-independent
voltage-transfer ratio," IEEE Trans. Power Electron., Vol.
29, No. 6, pp. 2979-2990, Jun. 2014.

[7] W. X. Zhong, C. Zhang, X. Liu, and S. Y. R. Hui, "A methodology for making a three-coil wireless power transfer system more energy efficient than a two-coil
Counter part for extended transfer distance," *IEEE Trans.*
Power Electron., Vol. 30, No. 2, pp. 933-942, Feb. 2015.

[8] X. Dai, Y. Zou, and Y. Sun, "Uncertainty modeling and robust control for LCL resonant inductive power transfer
system," *Journal of Power Electronics*, Vol. 13, No. 5, pp. 814-828, Sep. 2013.

[9] J. P. C. Smeets, T. T. Overboom, J. W. Jansen, and E. A. Lomonova, "Comparison of position-independent contactless energy transfer systems," *IEEE Trans. Power*
Electron., Vol. 28, No. 4, pp. 2059-2067, Apr. 2013.

[10] G. B. Joun and B. H. Cho, "An energy transmission system for an artificial heart using leakage inductance compensation of transcutaneous transformer," *IEEE Trans.*
Power Electron., Vol. 13, No. 6, pp. 1013–1022, Nov.1998.

[11] K. W. Klontz, D. M. Divan, D. W. Novotny, and R. D.
Lorenz, "Contactless power delivery system for mining applications," *IEEE Trans. Ind. Appl.*, Vol. 31, No. 1, pp. 27–35, Jan./Feb. 1995.

[12] J. Kuipers, H. Bruning, S. Bakker, and H. Rijnaarts, "Near field resonant inductive coupling to power electronic devices dispersed in water," *Sensors and Actuators A: Physical*, Vol. 178, pp. 217–222, May 2012.

[13] S. Hasanzadeh, S. Vaez-Zadeh, and A. H. Isfahani,
"Optimization of a contactless power transfer system for electric vehicles," *IEEE Trans. Veh. Technol.*, Vol. 61, No.

8, pp. 3566–3573, Oct. 2012.
[14] G. A. J. Elliot, S. Raabe, G. A. Covic, and J. T. Boys,
"Multiphase pickups for large lateral tolerance contactless power-transfer systems," *IEEE Trans. Ind. Electron.*, Vol.
57, No. 5, pp. 1590–1598, May 2010.
[15] J. Huh, S. W. Lee, W. Y. Lee, G. H. Cho, and C. T. Rim, "Narrow-width inductive power transfer system for online electrical vehicles," *IEEE Trans. Power Electron.*, Vol. 26, No. 12, pp. 3666–3679, Dec. 2011.
[16] B. Song, J. Shin, S. Lee, S. Shin, Y. Kim, S. Jeon, and G. Jung, "Design of a high power transfer pickup for on-line electric vehicle (OLEV)," in *IEEE International Electric Vehicle Conference (IEVC)*, pp. 1–4, Mar. 2012.
[17] K. D. Papastergiou and D. E. Macpherson, "An airborne radar power supply with contactless transfer of energy-part-I: Rotating transformer," *IEEE Trans. Ind. Electron.*, Vol. 54, No. 5, pp. 2874–2884, Oct. 2007.
[18] K. D. Papastergiou and D. E. Macpherson, "An airborne radar power supply with contactless transfer of energy-part-II: Converter design," *IEEE Trans. Ind.*
Electron., Vol. 54, No. 5, pp. 2885–2893, Oct. 2007.
[19] S. Chopra and P. Bauer, "Driving range extension of EV with on-road contactless power transfer—A case study," *IEEE Trans. Ind. Electron.*, Vol. 60, No. 1, pp. 329–338,
Jan. 2013.
[20] P. Si, A. P. Hu, S. Malpas, and D. Budgettt, "A frequency control method for regulating wireless power to
implantable devices," *IEEE Trans. Biomed. Circuits Syst.*,
Vol. 2, No. 1, pp. 22–29, Mar. 2008.
[21] J. H. Kim, B. S. Lee, J. H. Lee, S. H. Lee, C. B. Park, S. M. Jung, S. G. Lee, K. P. Yi, and J. Baek, "Development of 1MW inductive power transfer system for a high speed train," *IEEE Trans. Ind. Electron.*, Vol. 62, No. 10, pp. 6242-6250, Oct. 2015.
[22] A. P. Hu, *Selected resonant converters for IPT power supplies*, University of Auckland Digital Doctoral Theses, 2001.
[23] M. K. Kazimierczuk and D. Czarkowski, *Resonant power converters*, Second Edition, A John Wiley & Sons, Inc., Publication, 2012.
[24] A. Schonknecht and R. W. De Doncker, "Novel topology for parallel connection of soft-switching high-power high-frequency inverters," in *IEEE Industry Applications Conference*, Vol. 3, pp. 1477-1482, Sep./Oct. 2001.
[25] Z. J. Zhang, H. M. Li, Y. L. Peng, and Y. B. Li, "Phase shift control for multi-phase parallel LLC voltage-fed inverter," *Electronics Letters*, Vol. 46, No. 6, pp. 442–444, Mar. 2010.
[26] T. Mishima, C. Takami, and M. Nakaoka, "A new current phasorcontrolled ZVS twin half-bridge high-frequency resonant inverter for induction heating," *IEEE Trans. Ind. Electron.*, Vol. 61, No. 5, pp. 2531–2545, May 2014.
[27] H. Hao, G. A. Covic, and J. T. Boys, "A Parallel topology for inductive power transfer power supplies," *IEEE Trans. Power Electron.*, Vol. 29, No. 3, pp. 1140-1151, Mar. 2014.
[28] International Commission on Non-Ionizing Radiation Protection, "Guidelines for limiting exposure to time-varying electric and magnetic fields (1 Hz to 100
kHz)," *Health Physics*, Vol. 99, No. 6, pp. 818-836, Dec. 2010.
[29] N. Holtsmark and M Molinas, "Matrix converter efficiency in a high frequency link offshore WECS," in *37th Annual Conference on IEEE Industrial Electronics Society (IECON)*, pp. 1420-1425, Nov. 2011.
[30] Z. Ye, P. K. Jain, and P. C. Sen, "Circulating current minimization in high-frequency AC power distribution architecture with multiple inverter modules operated in parallel," *IEEE Trans. Ind. Electron.*, Vol. 54, No. 5, pp.
2673-2687, Oct. 2007.